Romanian participation at EUROfusion WPENR and complementary research / WPENR-RO

Project Director: Ion Tiseanu (INFLPR, ion.tiseanu@inflpr.ro)
Partner 1: Traian Petrisor (UTCN, traian.petrisorjr@phys.utcluj.ro)

The report is divided in four specific contributions:

I. **INFLPR: WP2 -Wire fabrication / Task 2.3: Microstructural characterization of the IBSC wires by X-ray microtomography**

The WP-ENR project "irOn-based supeRconducting wIres for fusiON" (ORION), CfP-FSD-AWP24-ENR-04, focuses on the development of iron-based superconducting (IBSC) wires using the Powder-In-Tube (PIT) method. The superconducting powders (Ba,K)Fe_2As_2 and $CaKFe_4As_4$ are used to establish a comprehensive fabrication process for these wires. Additionally, the project investigates innovative sheath materials—including Ta, Nb, and Ag-based alloys—to enhance wire performance.

The project is a collaboration among four research units: ENEA (coordinating institution), the SPIN-CNR Institute of the Italian National Research Council, the Technical University of Cluj-Napoca (TUCN), the National Institute for Laser, Plasma & Radiation Physics (INFLPR), and Roma Tre University. Morphological and structural characterization of the wires is performed using advanced microscopy and tomography techniques at the laboratories of CNR-SPIN, ENEA, and INFLPR.

INFLPR's contribution in 2025 centered on non-destructive microstructural evaluation using high-resolution X-ray microtomography (XCT) and radiography. This effort aims to establish benchmarks for the non-destructive testing of IBSC wires. During this reporting period, INFLPR performed extensive XCT analysis on:

$CaKFe_4As_4$ (1144) mono- and multifilamentary wires with Ta/Ta-alloy diffusion barriers (made by ENEA);
(Ba,K)Fe_2As_2 (122) composite-sheath tapes (CuNi/Nb/Ag) from ENEA and CNR-SPIN;
Single-wire and tape samples heat-treated at 800–900 °C.

INFLPR's 2025 activity consisted of:

1. Optimization of XCT scanning parameters for: Ta-sheathed 1144 wires; Composite CuNi/Nb/Ag 122 wires; Multifilamentary assemblies (MW01–MW03).
2. High-resolution microtomography (1.4–3.0 µm voxels) for: Barrier integrity assessment; Filament straightness and channel continuity; Crack quantification and defect morphology; Verification of densification and soldering patterns.
3. Radiography analysis for: Early crack detection; Mechanical stress evaluation in tapes following thermal cycling.

ENEA CaKFe4As4 Single and Multifilamentary Wires with Ta Diffusion Barrier

ENEA provided CaKFe4As4 wires with Ta diffusion barriers fabricated using various compacting methods:

- Groove-rolled square wires of 2.5 × 2.5 mm², 1.2 × 1.2 mm², and 0.8 × 0.8 mm².
- Flat-rolled wires of 2.0 × 0.8 mm².

The XCT analysis primarily focused on visualizing the microstructural integrity of the Ta barrier and its interaction with the external copper matrix and internal superconducting material.

Groove-rolled Wires: Manufacturing technology showed reliable results, with tolerable deviations in Ta barrier shape and integrity. The most compacted wires exhibited slight sausaging effects and internal dents.

Flat-rolled Wires: Tomography revealed limitations, likely due to strong mechanical interactions between the Ta barrier and the copper jacket.

Multifilamentary Wires: Additional challenges included geometrical complexity and Pb-based soldering of filaments. Despite this, XCT analysis satisfactorily assessed the Ta barrier's integrity and soldering quality. Notable findings included small penetrations in the Ta barrier and cavity patterns in the soldering material (Figure 1).

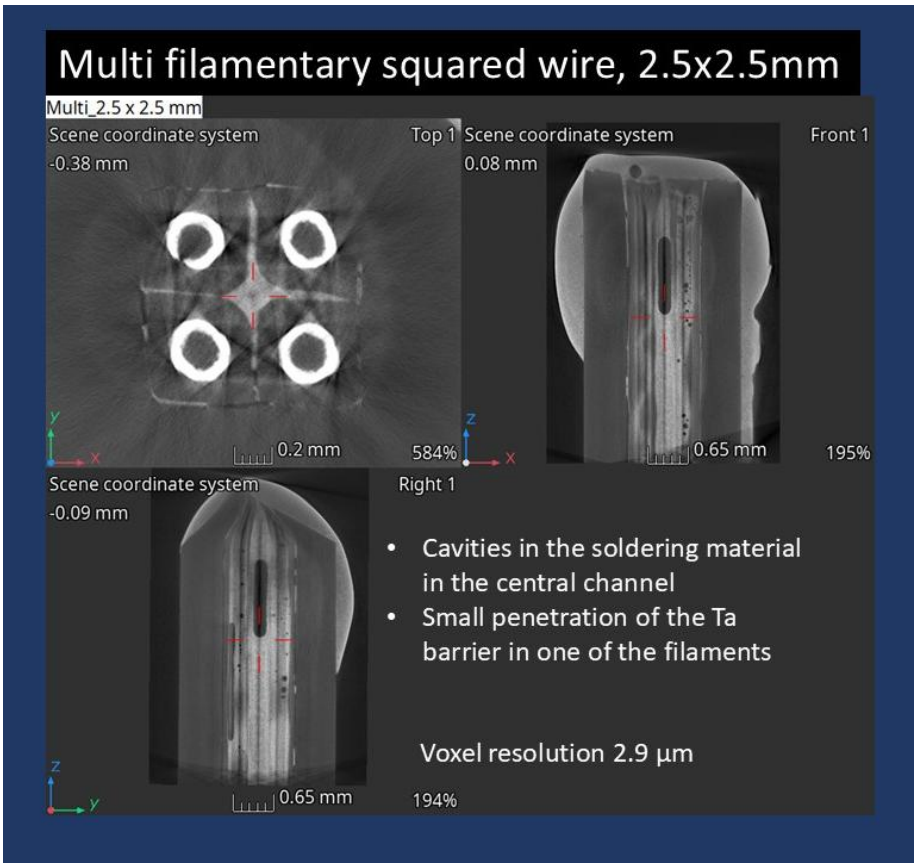

Figure 1. Tomography of a multifilamentary squared wire manufactured by ENEA. The microstructural integrity of the multiple Ta barriers and the quality of soldering can be satisfactorily assessed.

CNR-SPIN (Ba,K)Fe2As2 Single and Multifilamentary Wires with Silver Matrix

For CNR-SPIN's (Ba,K)Fe2As2 mono/multifilamentary wires with a silver matrix, the following experimental conditions were determined:

- **X-ray Source:** Operated at 170 kV and 80 µA with 0.05 mm Mo and Zr prefilters.
- **Detection System:** Large a-Si flat panel (4096 × 4096 pixels, 100 µm pixel size).
- **Scanning Configuration:** Nominal voxel resolution of 1.5 µm, suitable for tightly encapsulated samples.

CNR-SPIN provided flat-rolled wires in green and sintered forms, as well as square-shaped multifilamentary wires compacted from several flat-rolled wires. The XCT analysis highlighted:

Mono Wires: Excellent visualization of the silver jacket's integrity and interaction with the superconducting material. It seems that during the sintering process, there is a greater probability for

defects to occur. Although rare, these defects are in the form of thinning of the silver foil or even penetration.

Multifilamentary wires: XCT delivers highly resolved images in both green and sintered form. Most remarkable is the quality of the sintered structures and the delamination visualized inside the multilayer silver jacket (Figure 1).

The main advantage of the XCT analysis is that it offers easy access to many thousands of slices similar to the typical optical images. That allows, for example, to verify the straightness of the channels containing the superconductor material as shown in the axial cross sections shown in the middle of the montage.

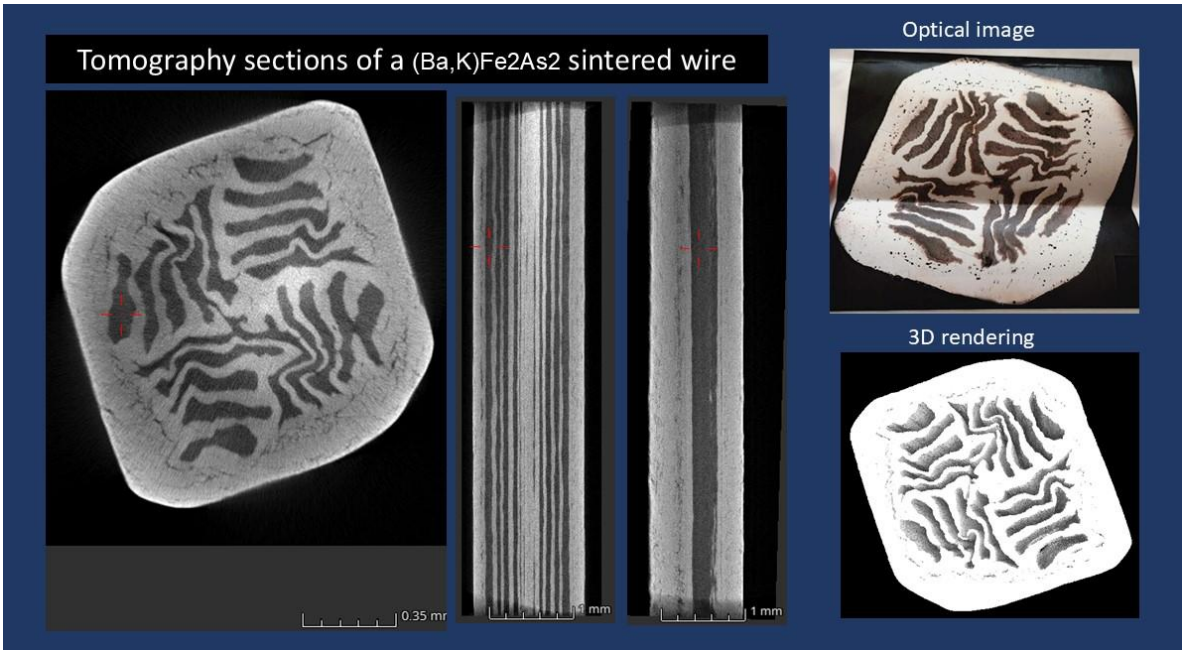

Figure 2. Tomography sections of a sintered multifilamentary (Ba, K)Fe2As2 wire with silver matrix and silver jacket.

The XCT analysis offered easy access to thousands of image slices, enabling thorough evaluations of features such as the straightness of superconducting material channels.

INFLPR provided high-fidelity XCT and radiography datasets for 1144 and 122 wires across all production stages.

Key findings:

• Ta barriers exhibit thinning, rupture, and sausaging during high-strain compaction;

• Composite tapes show thermally induced full-width cracks (5–37 μm);

• Silver-jacketed 122 wires exhibit sintering-induced thinning but improved filament alignment;

• Multifilamentary MW02–MW03 show promising structural consistency for scale-up;

Microtomography at INFLPR continues to serve as a benchmark for non-destructive evaluation of IBSC wires, informing sheath design, thermal routes, and mechanical processing strategies to support the development of high-performance, scalable wires for fusion applications.

II. INFLPR: Optimization of MgB_2 and of multilayer sheaths of IBSC Wires

The aim of the project is to assess the possibilities and limitations of using non-invasive X-ray imaging for characterization of MgB2 wires/tapes during their fabrication towards a better understanding of the complex relationship between processing processes and quality of the superconducting product.

Wires/tapes are fabricated by powder-in-tube technique. Namely, a powder of MgB2 or a 3D-printed stainless-steel structure with voids filled in with a MgB2 powder are introduced into seamless stainless-steel tubes. For reference, one sample is a tube loaded with the 3D-printed structure with voids, but without the MgB2 powder. Tubes are subject of multistep rolling steps. After certain processing steps, wires with a square cross section and tapes with a rectangular cross section are observed by X-ray imaging, namely by X-ray 3D radiography and 3D tomography. Geometrical details of the wires/tapes are revealed. The information allows monitoring and assessment of plastic deformation processes from the viewpoint of size, shape and defects aspects of each element composing the product, of their evolution during fabrication and of the interaction between the composing elements, e.g. between the core and the sheath. This information obtained after each processing step is extracted in a non-invasive manner and it can provide useful information for optimization of the processes and of the product. From a practical viewpoint, we found that there are limitations when applying many steps of deformation or when there is a subsequent change from square to flat rolling.

Presented aspects point on novel possibilities regarding fabrication and quality of the superconducting MgB2 wires, as well as on the need for further studies, seeking development of new statistical analysis methodologies based on X-ray imaging and of innovative approaches and concepts to integrate X-ray imaging in the fabrication and control processes.

Seamless stainless-steel tubes (Swagelok) were filled in with:

(i) MgB_2 powder (from LTS, USA) (Fig. 1(a)),

(ii) 3D-printed stainless-steel structure (Fig. 1(b)), and

(iii) 3D-printed stainless-steel structure filled in with MgB_2 powder. The filling of the 3D structure was carried out by inserting it into a thermoformable plastic holder with a special shape. The holder was then filled with an ultrasonicated solution of absolute ethyl alcohol (10 mL) and MgB_2 powder (1 g), and left to dry for 24 hours. After drying, approximately ~0.2 g of MgB_2 powder was present in the porous 3D structure. The 3D-printed structure has a diameter of 3.9 mm and a length of 5 cm.

XRT was applied using a metrologically-certified tomograph, built in house (Figure 3). It has a nano-focus X-ray tube with maximal working focal spot of 3 microns resolution, an X-ray detector (flat panel with 4096 x 4096 pixels,100 microns dimension, 16 bit resolution) and a Sigma Koki micron manipulator axis.

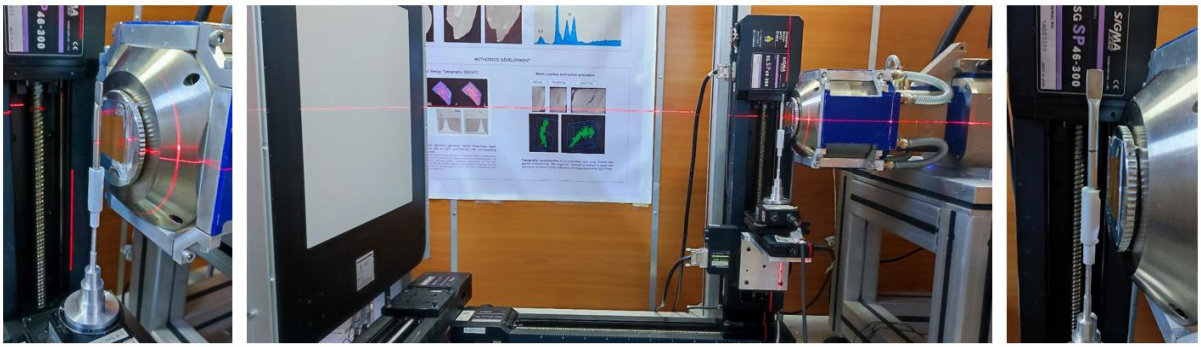

Figure 3 In-house built sub-micron Resolution Tomograph (up to 225 kV) with a Nanofocus X-ray source, 4k × 4k detector (100 µm pixels).

Two powder-in-tube wires with stainless steel sheath and MgB_2 core or with a core composed of a stainless-steel 3D-printed structure with voids filled in with MgB_2 powder were fabricated by square and flat rolling with subsequent heating using SPS technique. For reference, one wire had a core composed of

the 3D-printed structure with voids without MgB_2 powder. X-ray imaging, namely 2D radiography and 3D tomography, were performed after each deformation step and after SPS processing. Results indicate advanced possibilities to monitor and assess plastic deformation details from the viewpoint of size, shape and defects aspects of each element, of their evolution during fabrication and of the interaction between the core and sheath. This information is obtained after each processing step, this is achieved in a non-invasive manner and can provide useful information for optimization of the processes and of the product. From a practical viewpoint, we found that there are limitations when applying many steps of deformation or when there is a subsequent change from square to flat rolling. Presented aspects point on novel possibilities regarding fabrication and quality of the superconducting MgB_2 wires, as well as on the need for further studies, seeking development of new statistical analysis methodologies based on X-ray imaging and of innovative approaches and concepts to integrate X-ray imaging in the fabrication and control processes.

III. UTCN- Partner 1: Development of novel sheath material for iron-based superconducting (IBS) cables

The project aims to develop a novel sheath material for iron-based superconducting (IBS) cables, focusing on Ag-coated Cu foils as a promising architecture for PIT-processed wires. A key aspect is optimizing the electroplating process to obtain Ag films with suitable mechanical and electrical properties. To complement standard thin-film characterization techniques (XRD, AFM, resistivity), the work implements temperature-dependent low-frequency noise spectroscopy as a diagnostic for film quality. By analyzing the 1/f noise component, this method sensitively probes defect dynamics, grain boundary stability, and diffusion mechanisms, allowing early prediction of electromigration-related failure well before resistance changes become apparent. Different activation energy ranges can be linked to specific processes, such as surface or grain-boundary diffusion, giving deeper insight into film microstructure and defect chemistry.

To enable these measurements, three low-noise amplification systems were designed and characterized using two biasing schemes: a voltage divider and a Wheatstone bridge. All systems use two-channel cross-correlation, careful PCB design, and shielding to achieve ~60 dB gain, sub-nV/√Hz baseline noise, and bandwidths suitable for low-frequency noise spectroscopy. In the voltage-divider configuration, two amplifier chains were built: a low-noise op-amp-based LNA and a JFET–op-amp hybrid ULNA, the latter achieving a white noise floor of ~0.1 nV/√Hz after cross-correlation, comparable to state-of-the-art designs. The Wheatstone-bridge approach, read out by an instrumentation amplifier, is optimized to isolate the sample's 1/f noise by subtracting spectra with and without bridge excitation, making it particularly useful when the selective characterization of defect-related noise is desired. Together, these amplification systems provide a robust toolkit for high-sensitivity noise-based evaluation of electroplated Ag films for advanced superconducting cable technologies.

The work reports the design, implementation, and characterization of three low-noise amplification systems for electronic noise measurements, using two different biasing configurations: a voltage divider and a Wheatstone bridge. In all cases, a two-channel cross-correlation scheme was adopted to suppress uncorrelated amplifier noise. The amplifiers are battery-powered and operated inside a shielded, anechoic environment. The PCBs were designed as four-layer boards with solid inner ground and power planes and extensive via-stitch shielding, effectively forming a Faraday cage around sensitive traces. Careful layout

(short input loops, local decoupling, thermal management of op-amps) further reduced electromagnetic interference and ensured stable operation across the low-frequency band of interest (<1 Hz–100 kHz).
In the first approach, the sample was biased in a voltage-divider configuration with a large, low-noise series resistor, chosen such that the equivalent resistance matched the sample. A passive high-value R1–C1 AC-coupling network removed the DC component at the amplifier input while introducing a negligible noise contribution above the measurement band's low-frequency limit. Detailed noise modeling of the capacitor's leakage and series resistance showed that the stop-band noise floor of this filter is set by the thermal noise of the capacitor's ESR, establishing the lower bound for the system's achievable background noise.

Two amplification chains were realized for the voltage-divider scheme.
1. The "LNA" is a two-stage non-inverting amplifier based on ADA4625 op-amps. Component values were selected so that the input-referred thermal noise of the feedback networks remained below the intrinsic op-amp voltage noise (3.3 nV/√Hz), making the first stage's input voltage noise the dominant contribution. The measured passband gain of this system was ~61 dB over 12 mHz–220 kHz, with a single-channel background of ~3.2 nV/√Hz that was reduced to ~0.6 nV/√Hz by cross-correlation.

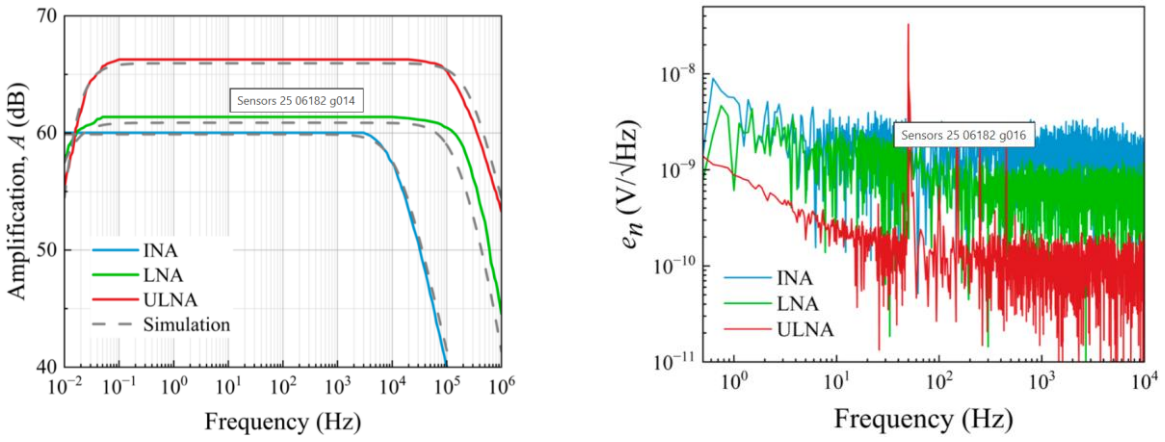

(a) (b)

Figure 2. (a) Measured and simulated amplification of the three different systems (INA, LNA, ULNA), and their corresponding bandwidths; (b) Cross-correlation spectra of the three amplification configurations.

2. The "ULNA" employs a hybrid front end consisting of eight JFETs (2SK3557) in parallel in a common-source configuration, coupled to a transimpedance stage based on an LT1028 op-amp, followed by a low-noise ADA4625 non-inverting stage. Parallelizing the JFETs increases the effective transconductance and decreases the input-referred channel noise by √N, while shot noise from the gate leakage current is negligible. Noise analysis shows that the common-source stage dominates the total noise budget, with the subsequent op-amp stages giving much smaller contributions once referred to the input. The calibrated passband gain of this ULNA chain is ~66 dB over 24 mHz–178 kHz, with a single-channel white noise floor of ~0.54 nV/√Hz above 100 Hz, reduced to ~0.1 nV/√Hz after cross-correlation—comparable to the best published ultra-low-noise designs.
In the second approach, the sample was embedded in a quarter-bridge Wheatstone configuration, with the sample and a low-noise wire-wound potentiometer forming the lower arms and high-value metal-foil ballast resistors forming the upper arms. By recording spectra with and without bridge excitation and

subtracting them, the authors derive an expression that isolates the sample's 1/f contribution while canceling the thermal noise of the resistive elements; this is a key conceptual difference from the voltage-divider method, which measures both 1/f and thermal components simultaneously. The Wheatstone bridge output is read by an LT1167 instrumentation amplifier. With a gain of 60 dB, the measured single-channel input-referred noise is ~8.9 nV/√Hz at 1 kHz, reduced to ~1.59 nV/√Hz using cross-correlation. A systematic study versus source resistance from 10 Ω to 1 MΩ shows that, for kΩ-range sources such as the investigated device (~2.26 kΩ), the amplifier operates in a regime where the sample thermal noise dominates over both voltage and current noise of the INA, validating its suitability for Wheatstone-bridge read-out.

Conclusion

Overall, the results demonstrate that all three amplification systems meet the design targets of ~60 dB gain, sub-nV/√Hz baseline noise (with cross-correlation) and appropriate bandwidth for low-frequency electronic noise measurements on single magnetoresistive elements. Among them, the voltage-divider configuration with the ULNA front end provides the lowest achievable background and is therefore the most promising choice when characterizing sample with particularly low intrinsic noise, whereas the Wheatstone-bridge plus INA scheme is especially advantageous when selective measurement of the 1/f component is desired.

IV. UTCN- Partner 1: WP1: Material properties/Task 1.3: Sheath development and production

This report presents the activities related to the development of Ta-based alloys and the mechanical characterization of Ta–W foils for sheath applications in iron-based superconducting (IBS) cable production. The Ta-based alloys were synthesized by plasma arc melting, and the Ta–W foils were subsequently evaluated by tensile strength testing to assess their suitability for demanding mechanical and thermal conditions. The sheath plays a critical role, providing mechanical support, chemical stability, and thermal management, with tantalum (Ta) and Ta–W alloys being particularly valuable candidates due to their high strength and excellent corrosion resistance.

In parallel, an alternative route was also explored. Austenitic stainless steels, particularly 316L, offer an attractive option because they are readily available, mechanically robust, and exhibit mechanical properties comparable to Ta and Ta-based alloys. However, stainless steel is more chemically reactive with IBS core materials and lacks a naturally compatible interface. To address this challenge, a surface conversion layer obtained by phosphating is investigated as a potential diffusion barrier and adhesion-promoting layer between the stainless-steel sheath and the iron-based superconducting core.

Overall, the activities carried out on Ta–W and Ta–Nb alloys have established a solid experimental basis for their use as sheath materials in iron-based superconducting cables. Arc-furnace synthesis successfully produced compositionally controlled Ta–W and Ta–Nb alloys. However, subsequent heat treatment optimization is still needed to avoid cracking and obtain microstructures suitable for rolling into foils. In parallel, tensile testing of commercial Ta–W foils provided valuable benchmarks for strength behavior under load. Together, these results demonstrate that Ta-based alloys can combine the mechanical robustness and thermal stability required for sheath applications, while also identifying key processing parameters and microstructural features that must be controlled to ensure reliable performance in IBS cable fabrication and operation.

Alternatively, to Ta-based foil approach, a phosphating process for stainless steel foils has been developed and assessed as a potential route to engineer sheath materials for iron-based superconducting cables. The formation of a stable phosphate conversion layer was demonstrated. The coating shows good adhesion and uniform phosphorus distribution across the surface. The phosphate layer remains stable after annealing up to 1050 °C and survives lamination from 0.5 mm to 0.28 mm without significant morphological degradation, indicating strong mechanical robustness. From a mechanical standpoint, phosphated stainless steel foils could provide a scalable, cost-effective alternative to Ta-based foils for IBS sheaths. However, the critical issue of chemical compatibility with IBS cores remains unresolved and must be thoroughly investigated before industrial implementation. Additionally, the phosphate layer suffers from low electrical and thermal conductivity, which are needed from the sheath to provide thermal and electrical runways in case of quenching of the IBS core. However, the present findings may still find application in the IBS powder synthesis. A phosphating layer may prove to be beneficial in the case when the superconducting powders are synthesized in stainless steel reactors.

Papers

C. Davidaș, E. M. Ștețco, L. M. Viman, M. S. Gabor, O. A. Pop, and T. Petrișor, ”Electronic Noise Measurement of a Magnetoresistive Sensor: A Comparative Study”, *Sensors* **25(19)**, 6182 (2025)

Conferences

Giuseppe Celentano, Gabriele Colombo, Valentina Corato, Gianluca De Marzi, Andrea Formichetti, Ferruccio Maierna, Marcello Marchetti, Andrea Masi, Lucio Merli, Luigi Muzzi, Alessandro Rufoloni, Angelo Vannozzi, Marco Breschi, Ion Tiseanu, Analysis of the Quench Experiment on the Aluminum slotted-core HTS conductors 17th European Conference on Applied Superconductivity, 21-25 September 2025, Porto

Meetings

10.06.2025, Cluj-Napoca (Romania), Technical University of Cluj-Napoca (TUCN) – ORION Project - Progress Meeting

14.10.2025, Online Meeting, ORION teams fall meeting

9-10.12.2025, Frascati/Roma (Italia), ENEA, Nuclear Department, Frascati, Italy, ORION Final meeting